

**Boulder School for
Condensed Matter and Materials Physics**

**Laurette Tuckerman
PMMH-ESPCI-CNRS
laurette@pmmh.espci.fr**

**Hydrodynamic Instabilities:
Open Flows**

This chapter summarizes parts of the following textbook and review article:

- P. J. Schmid & D. S. Henningson, *Stability and Transition in Shear Flows*, Springer, 2001.
- P. Huerre & M. Rossi, *Hydrodynamic instabilities in open flow*, in *Hydrodynamics and Nonlinear Instabilities*, ed. C. Godrèche & P. Manneville, Cambridge University Press, 1998.

References to the original bibliography follows the text.

1 Plane parallel flows

1.1 Introduction

We analyze the linear stability of a plane parallel flow $\mathbf{U} = U(y)\mathbf{e}_x$. The usual nomenclature is:

x	main flow direction	streamwise
y	between the bounding plates	cross-channel
z		spanwise

Plane parallel flows are easy to formulate, since they are incompressible by construction and the nonlinear term in the Navier-Stokes vanishes.

$$\begin{aligned} (\mathbf{U} \cdot \nabla)\mathbf{U} &= (U(y)\mathbf{e}_x \cdot \nabla)U(y)\mathbf{e}_x = U(y)\partial_x U(y)\mathbf{e}_x = 0 \\ \nabla \cdot U(y)\mathbf{e}_x &= \partial_x U(y) = 0 \end{aligned} \quad (1)$$

The remaining equation that U must satisfy is:

$$0 = -\nabla P + \frac{1}{R}\Delta\mathbf{U} = \begin{cases} -\partial_x P + \frac{1}{R}U''(y) \\ -\partial_y P \\ -\partial_z P \end{cases} \quad (2)$$

Since $\partial_x P$ depends only on y and $\partial_y P = 0$, then $\partial_x P$ must be a constant, which we will call $-G$. For inviscid (ideal) fluids, $R = \infty$ and then all functions $U(y)$ are allowed. For viscous fluids, we must solve

$$\begin{aligned} 0 &= G + \frac{1}{R}U''(y) \\ U(y) &= -\frac{GR}{2}y^2 + ay + b \end{aligned} \quad (3)$$

1.2 Poiseuille and Couette flow

Two well-known examples are Poiseuille and Couette flow in a channel bounded by $-1 \leq y \leq +1$. For Poiseuille flow, the boundaries are stationary, so that $U(\pm 1) = 0$, leading to

$$U(y) = \frac{GR}{2}(1 - y^2) \quad (4)$$

In Couette flow, the pressure gradient G is zero and the flow is driven by the motion of the boundaries at different speeds. We can always go into a moving frame such that $U(\pm 1) = \pm 1$, leading to:

$$U(y) = y \quad (5)$$

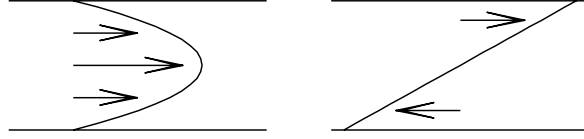


Figure 1: Plane Poiseuille flow (left) and plane Couette flow (right).

Poiseuille and Couette flow, as well as the analogous problem of pressure-driven pipe flow ($U(z) = 1 - r^2$) all display the same behavior: they undergo a sudden transition to three-dimensional turbulence. Yet, at the Reynolds numbers at which this transition takes place, all three flows are linearly stable.

1.3 Reduction to two variables

We now study the behavior of perturbations $\mathbf{u} = (u, v, w)$ to a plane parallel flow. The nonlinear term linearized about such a flow is:

$$\begin{aligned} (\mathbf{U} \cdot \nabla) \mathbf{u} &= (U(y) \mathbf{e}_x \cdot \nabla) \mathbf{u} = U(y) \partial_x \mathbf{u} \\ (\mathbf{u} \cdot \nabla) \mathbf{U} &= (\mathbf{u} \cdot \nabla) U(y) \mathbf{e}_x = v U'(y) \mathbf{e}_x \end{aligned} \quad (6)$$

The linearized Navier-Stokes equations become:

$$\partial_t \mathbf{u} + U \partial_x \mathbf{u} + v U' \mathbf{e}_x = -\nabla p + \frac{1}{R} \Delta \mathbf{u} \quad (7)$$

$$\nabla \cdot \mathbf{u} = 0 \quad (8)$$

We wish to reduce this system of four equations in four variables (u, v, w, p) to two equations in two variables, which will be the velocity v and vorticity η in the y direction. We begin by taking the divergence of (7) so as to eliminate the pressure:

$$\nabla \cdot \partial_t \mathbf{u} + \nabla \cdot (U \partial_x \mathbf{u}) + \nabla \cdot (v U' \mathbf{e}_x) = \nabla \cdot (-\nabla p) + \nabla \cdot \left(\frac{1}{R} \Delta \mathbf{u} \right) \quad (9)$$

Calculating the individual terms of (9) and using (8)

$$\begin{aligned} \nabla \cdot \partial_t \mathbf{u} &= \partial_t \nabla \cdot \mathbf{u} = 0 \\ \nabla \cdot (U \partial_x \mathbf{u}) &= U \nabla \cdot (\partial_x \mathbf{u}) + (\nabla U) \cdot \partial_x \mathbf{u} = U \partial_x \nabla \cdot \mathbf{u} + U' \partial_x v = U' \partial_x v \\ \nabla \cdot (v U' \mathbf{e}_x) &= \partial_x (v U') = U' \partial_x v \\ \nabla \cdot (-\nabla p) &= -\Delta p \\ \nabla \cdot \left(\frac{1}{R} \Delta \mathbf{u} \right) &= \frac{1}{R} \Delta \nabla \cdot \mathbf{u} = 0 \end{aligned}$$

leads to

$$2U'\partial_x v = -\Delta p \quad (10)$$

We now take the Laplacian of the y component of (7):

$$\Delta\partial_t v + \Delta(U\partial_x v) = -\Delta\partial_y p + \frac{1}{R}\Delta^2 v \quad (11)$$

We expand the terms in the middle of (11):

$$\begin{aligned} \Delta(U\partial_x v) &= U\Delta\partial_x v + 2U'\partial_{xy}v + U''\partial_x v \\ -\Delta\partial_y p &= \partial_y(2U'\partial_x v) = 2U'\partial_{xy}v + 2U''\partial_x v \end{aligned}$$

to arrive at our first equation, which contains only v :

$$(\partial_t + U\partial_x)\Delta v = U''\partial_x v + \frac{1}{R}\Delta^2 v \quad (12)$$

The second equation is obtained by taking the y component of the curl of (7):

$$\mathbf{e}_y \cdot \nabla \times (\partial_t \mathbf{u} + U\partial_x \mathbf{u} + vU'\mathbf{e}_x) = \mathbf{e}_y \cdot \nabla \times \left(-\nabla p + \frac{1}{R}\Delta \mathbf{u} \right) \quad (13)$$

We define

$$\eta \equiv \mathbf{e}_y \cdot \nabla \times \mathbf{u} = \partial_z u - \partial_x w \quad (14)$$

and calculate the terms of (13):

$$\begin{aligned} \mathbf{e}_y \cdot \nabla \times \partial_t \mathbf{u} &= \partial_t \eta \\ \mathbf{e}_y \cdot \nabla \times (U\partial_x \mathbf{u}) &= \partial_z(U\partial_x u) - \partial_x(U\partial_x w) = U\partial_{xz}u - U\partial_{xx}w = U\partial_x \eta \\ \mathbf{e}_y \cdot \nabla \times (vU'\mathbf{e}_x) &= \partial_z(vU') = U'\partial_z v \\ \mathbf{e}_y \cdot \nabla \times (-\nabla p) &= 0 \\ \mathbf{e}_y \cdot \nabla \times \left(\frac{1}{R}\Delta \mathbf{u} \right) &= \frac{1}{R}\Delta \eta \end{aligned}$$

This gives us a second equation, which couples η and v :

$$(\partial_t + U\partial_x)\eta + U'\partial_z v = \frac{1}{R}\Delta \eta \quad (15)$$

Equations (12) and (15) require boundary conditions. We assume periodic boundary conditions in x and z . In y , equation (12) is of 4th order in v and thus requires 4 boundary conditions on v , while equation (15) is of 2nd order in η , requiring 2 boundary conditions on η . These boundary conditions are applied at $y = y_{\pm}$, where y_{\pm} can be finite or infinite. We have

$$v = 0 \text{ at } y = y_{\pm} \quad (16)$$

We transform the boundary conditions $u = w = 0$ at $y = y_{\pm}$ to conditions on v and η as follows:

$$\partial_x u = \partial_z w = 0 \implies \partial_y v = 0 \quad (17)$$

$$\partial_z u = \partial_x w = 0 \implies \eta = 0 \quad (18)$$

1.4 Orr-Sommerfeld and Squire equations

The linear system (12), (15) with boundary conditions (16)-(18) is *homogeneous* in x, z, t ; that is, neither the equations nor the boundary conditions distinguish between different values of x, z, t . In contrast, the system is not homogeneous in y , both because the plane parallel flow $U(y)$ whose stability is being studied depends on y and also because the boundary conditions distinguish between different values of y : we can be closer or farther from the boundaries. Linear systems which are homogeneous in some of their independent variables have as their solutions functions which are exponential or trigonometric in these variables:

$$v(x, y, z, t) = \hat{v}(y)e^{i(\alpha(x-ct)+\beta z)} \quad (19)$$

$$\eta(x, y, z, t) = \hat{\eta}(y)e^{i(\alpha(x-ct)+\beta z)} \quad (20)$$

We seek solutions which are bounded in x, z , in which case the wavenumbers α, β are real. In contrast, we do not specify whether c is real, imaginary, or complex. This is precisely what will distinguish between flows \mathbf{U} which are stable or unstable. The convention in this field is to write the time dependence as $\exp(-i\alpha ct)$. With α real, this convention means that c_i is the *growth rate*: perturbations v, η grow if $c_i > 0$, decay if $c_i < 0$, and are neutral if $c_i = 0$. The value of c_r gives the *phase speed*: a peak moves at speed c_r .

By substituting (19)-(20) into equations (12) and (15), and defining $D \equiv d/dy$ and $k^2 \equiv \alpha^2 + \beta^2$, we obtain:

$$(-i\alpha c + U i\alpha)(D^2 - k^2)\hat{v} = U'' i\alpha \hat{v} + \frac{1}{R}(D^2 - k^2)^2 \hat{v} \quad (21)$$

$$-i\alpha c \hat{\eta} + U i\alpha \hat{\eta} + U' i\beta \hat{v} = \frac{1}{R}(D^2 - k^2)\hat{\eta} \quad (22)$$

Dividing by $i\alpha$:

$$(U - c)(D^2 - k^2)\hat{v} = U'' \hat{v} + \frac{1}{Ri\alpha}(D^2 - k^2)^2 \hat{v} \quad (23)$$

$$(U - c)\hat{\eta} + U' \frac{\beta}{\alpha} \hat{v} = \frac{1}{Ri\alpha}(D^2 - k^2)\hat{\eta} \quad (24)$$

Equations (23)-(24) with (16)-(18) constitute an eigenvalue problem with eigenvalues c and eigenvectors $\hat{v}, \hat{\eta}$. Equation (23) for \hat{v} is called the *Orr-Sommerfeld equation* [1, 2] and equation (24) coupling \hat{v} and $\hat{\eta}$ is called *Squire's equation* [3].

For inviscid fluids ($R = \infty$), the coefficients in (23)-(24) are all real. This implies that the eigenvalues c are either real (a neutral perturbation, which neither grows nor decays), or complex conjugates (one growing and one decaying perturbation). This is a property of inviscid fluids and of conservative problems in general: since volumes must be conserved, growth in one direction must be compensated by decay in another. In conservative systems, most perturbations are neutral, possibly oscillating, but

neither growing nor decaying. Such systems become unstable when two neutral eigenvalues merge at zero to become a growing/decaying pair. In contrast, in non-conservative systems, most perturbations decay, and instability arises when one or more eigenvalues cross zero to become growing perturbations.

The system (23)-(24) can be written in matrix form as:

$$\begin{aligned} \begin{bmatrix} 0 \\ 0 \end{bmatrix} &= \begin{bmatrix} [(U - c) - \frac{1}{Ri\alpha}(D^2 - k^2)](D^2 - k^2) - U'' & 0 \\ U' \frac{\beta}{\alpha} & (U - c) - \frac{1}{Ri\alpha}(D^2 - k^2) \end{bmatrix} \begin{bmatrix} \hat{v} \\ \hat{\eta} \end{bmatrix} \\ &\equiv \begin{bmatrix} \mathcal{L}_{OS} & 0 \\ B & \mathcal{L}_{SQ} \end{bmatrix} \begin{bmatrix} \hat{v} \\ \hat{\eta} \end{bmatrix} \end{aligned} \quad (25)$$

This system is upper triangular. Its eigenvalues and eigenvectors can be divided into two families, the *Orr-Sommerfeld modes* and the *Squire modes*:

$$\begin{aligned} \text{Modes OS : } \quad \mathcal{L}_{OS}\hat{v} = 0, \hat{v} \neq 0 \\ \mathcal{L}_{SQ}\hat{\eta} = -B\hat{v} \end{aligned} \quad \text{Modes SQ : } \quad \hat{v} = 0 \\ \mathcal{L}_{SQ}\hat{\eta} = 0, \hat{\eta} \neq 0 \quad (26)$$

The Squire modes are always neutral for inviscid fluids ($R = \infty$), and damped for viscous fluids. We show this by writing:

$$\begin{aligned} 0 &= \left(U - c - \frac{1}{Ri\alpha}(D^2 - k^2) \right) \hat{\eta} \\ 0 &= \int dy \hat{\eta}^* \left(U - c - \frac{1}{Ri\alpha}(D^2 - k^2) \right) \hat{\eta} \\ &= \int dy U |\hat{\eta}|^2 - c \int dy |\hat{\eta}|^2 - \frac{1}{Ri\alpha} \int dy \hat{\eta}^* D^2 \hat{\eta} + \frac{k^2}{Ri\alpha} \int dy |\hat{\eta}|^2 \end{aligned} \quad (27)$$

Integration by parts yields:

$$\int_{-1}^{+1} dy \hat{\eta}^* D^2 \hat{\eta} = \hat{\eta}^* D\hat{\eta} \Big|_{-1}^{+1} - \int_{-1}^{+1} dy |D\hat{\eta}|^2 \quad (28)$$

where the surface term disappears because of the boundary conditions $\hat{\eta}(\pm 1) = 0$. The imaginary part of (27) is thus:

$$c_i \int dy |\hat{\eta}|^2 = -\frac{1}{R\alpha} \int dy |D\hat{\eta}|^2 - \frac{k^2}{R\alpha} \int dy |\hat{\eta}|^2 \leq 0 \quad (29)$$

To seek linear instabilities, we therefore study the Orr-Sommerfeld equation and its eigenmodes.

1.5 Squire's Transformation

A very well-known result about the Orr-Sommerfeld equation is called *Squire's Theorem* [3]. We define

$$\tilde{\alpha}^2 \equiv \alpha^2 + \beta^2 \quad (30)$$

$$\tilde{\beta} \equiv 0 \quad (31)$$

$$\tilde{R} \equiv R\alpha/\tilde{\alpha} \quad (32)$$

and substitute into equation (23):

$$(U - c)(D^2 - \tilde{\alpha}^2)\hat{v} = U''\hat{v} + \frac{1}{\tilde{R}i\tilde{\alpha}}(D^2 - \tilde{\alpha}^2)^2\hat{v} \quad (33)$$

We see that (23) is also an Orr-Sommerfeld equation, with an increased wavenumber in x , a zero wavenumber in z (the perturbation is independent of z), a decreased Reynolds number, and an unchanged c and \hat{v} .

In the case of a viscous fluid, we assume that there is no instability for low Reynolds number. With fixed α, β we increase R until one of the c_i becomes positive, meaning \mathbf{U} has become unstable. Squire's Theorem states that the wavenumbers $\tilde{\alpha}, \tilde{\beta} = 0$ lead to instability for \tilde{R} , which is less than R . To find the lowest Reynolds number for which (23) becomes unstable, it is therefore sufficient to consider two-dimensional cases, with $\beta = 0$. In the case of an inviscid fluid, Squire's Theorem states that the problem with $\alpha, \beta > 0$ is identical to that with $\tilde{\alpha}, \tilde{\beta} = 0$, and hence, again, we can set $\beta = 0$.

The problem of the stability of plane parallel flows has been greatly simplified. In section 1.3, we reduced the Navier-Stokes equations (four equations coupling four fields u, v, w, p) to two equations in v, η . In section 1.4, by choosing wavenumbers α and β and wavespeed c , we reduced the partial differential equations in x, y, z, t first to a pair of ordinary differential equations in y , and then to the Orr-Sommerfeld equation alone. Finally, here in section 1.5, we eliminated one of the wavenumbers, leading to a single equation relating c to R and k . Because of these successive simplifications, it has been possible to prove rigorously that Poiseuille and Couette flow are linearly stable in the Reynolds numbers range in which transition to turbulence occurs, both experimentally and numerically.

At this time, there is no definite resolution to this dilemma, but we will address some possible approaches in section 3.

2 Classical theory of ideal fluids

2.1 Rayleigh Equation

In the framework of ideal (inviscid) fluids, the Orr-Sommerfeld equation is called *the Rayleigh equation* [4, 5].

$$[(U - c)(D^2 - k^2) - U''] \hat{v} = 0 \quad (34)$$

We will now demonstrate several classical properties of (34). The first is *Rayleigh's inflection point theorem* (1880), which states that $c_i \neq 0$, then $U(y)$ has an inflection point. This means that if $U(y)$ does *not* have an inflection point, then $c_i = 0$ and so U is stable. We show this as follows. Starting from (34), we divide by $-(U - c)$ (since $(U - c) \neq 0$ if $c_i \neq 0$); we multiply by \hat{v}^* , the complex conjugate of \hat{v} ,

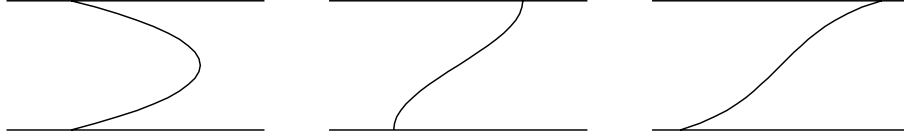


Figure 2: Three velocity profiles. Left: this profile does not have an inflection point $U''(y_S) = 0$, and is therefore stable according to Rayleigh's criterion. Middle: this profile has an inflection point and thus could be unstable according to Fjortoft's criterion. Right: this profile has an inflection point which implies a stable flow according to Fjortoft's criterion.

and we integrate over $[-1, 1]$:

$$0 = \int_{-1}^{+1} dy \hat{v}^* \left[(-D^2 + k^2) + \frac{U''}{U - c} \right] \hat{v} \quad (35)$$

We rewrite (35) using integration by parts as we did in (28):

$$\begin{aligned} 0 &= \int_{-1}^{+1} dy \left[|D\hat{v}|^2 + k^2|\hat{v}|^2 + \frac{U''}{U - c}|\hat{v}|^2 \right] \\ &= \int_{-1}^{+1} dy \left[|D\hat{v}|^2 + k^2|\hat{v}|^2 + \frac{U''(U - c_r)}{|U - c|^2}|\hat{v}|^2 \right] + ic_i \int_{-1}^{+1} dy \frac{U''}{|U - c|^2}|\hat{v}|^2 \end{aligned} \quad (36)$$

For the imaginary part of the right-hand-side of (36) to be zero, the integral multiplying c_i must be zero (since $c_i \neq 0$). For this to happen, U'' must change sign over $[-1, +1]$, and thus U must have an inflection point y_S where $U''(y_S) = 0$.

Fjortoft's Theorem [6] refines the inflection point criterion: if $c_i \neq 0$, then $U''(y)(U(y) - U(y_S))$ must be negative over a portion of the interval $[-1, +1]$. Let us rewrite the real part of (36):

$$\int_{-1}^{+1} dy \frac{U''(U - c_r)}{|U - c|^2}|\hat{v}|^2 = - \int_{-1}^{+1} dy [|D\hat{v}|^2 + k^2|\hat{v}|^2] < 0 \quad (37)$$

We define $U_S \equiv U(y_S)$ and multiply the imaginary part of (36) by $(c_r - U_S)/c_i$:

$$\int_{-1}^{+1} dy \frac{U''(c_r - U_S)}{|U - c|^2}|\hat{v}|^2 = 0 \quad (38)$$

We add (37) and (38):

$$\int_{-1}^{+1} dy \frac{U''(U - c_r + c_r - U_S)}{|U - c|^2}|\hat{v}|^2 = - \int_{-1}^{+1} dy [|D\hat{v}|^2 + k^2|\hat{v}|^2] < 0 \quad (39)$$

We therefore have:

$$\int_{-1}^{+1} dy \frac{U''(U - U_S)}{|U - c|^2} |\hat{v}|^2 < 0 \quad (40)$$

which requires that $U''(y)(U - U_S)$ be negative over a portion of the interval. Note that the Rayleigh and Fjortoft criteria apply only to inviscid fluids and can only demonstrate stability and not instability.

Howard's semicircle theorem [7] states that the unstable eigenvalues of the Rayleigh equation obey:

$$\left(c_r - \frac{1}{2}(U_{\max} + U_{\min}) \right)^2 + c_i^2 \leq \frac{1}{2}(U_{\max} - U_{\min})^2 \quad (41)$$

In other words, they are located inside the circle whose diameter is the line segment between U_{\max} and U_{\min} . We will not prove this theorem.

2.2 Kelvin-Helmholtz Instability

The Kelvin-Helmholtz instability arises from a velocity gradient. Let us first apply Rayleigh's equation to the Kelvin-Helmholtz instability. To do so, we will study the stability of piecewise-constant profiles on the domain $-\infty < y < \infty$. For this case, we must specify jump conditions at each discontinuity of U . The first condition is:

$$\left. \frac{\hat{v}}{U - c} \right] = 0 \quad (42)$$

where $]$ means the difference in the quantity evaluated on either side of the discontinuity. This condition insures that the interface between the two sides remains well-defined. The second condition is:

$$((U - c)D - U')\hat{v}] = 0 \quad (43)$$

This condition insures the continuity of the normal stress (the pressure). Let us now consider the simplest profile:

$$U = \begin{cases} U_+ & \text{for } y > 0 \\ U_- & \text{for } y < 0 \end{cases} \quad (44)$$

In each of the two domains, Rayleigh's equation (34) has the form

$$(D^2 - k^2)\hat{v} = 0 \quad (45)$$

Given the boundary conditions $\hat{v} = 0$ at $y = \pm\infty$, the solution is

$$\hat{v} = \begin{cases} Ae^{-ky} & \text{for } y > 0 \\ Be^{ky} & \text{for } y < 0 \end{cases} \quad (46)$$

We apply the jump conditions at $y = 0$:

$$0 = \frac{\hat{v}}{U_- - c}(0^+) - \frac{\hat{v}}{U_- - c}(0^-) = \frac{A}{U_+ - c} - \frac{B}{U_- - c} \quad (47)$$

$$\begin{aligned} 0 &= ((U - c)D - U')\hat{v}(0^+) - ((U - c)D - U')\hat{v}(0^-) \\ &= (U_+ - c)(-kA) - (U_- - c)kB \end{aligned} \quad (48)$$

or

$$\begin{bmatrix} 0 \\ 0 \end{bmatrix} = \begin{bmatrix} \frac{1}{U_+ - c} & \frac{-1}{U_- - c} \\ (U_+ - c) & (U_- - c) \end{bmatrix} \begin{bmatrix} A \\ B \end{bmatrix} \quad (49)$$

A non-trivial solution exists if the determinant is zero:

$$\begin{aligned} 0 &= \frac{U_- - c}{U_+ - c} + \frac{U_+ - c}{U_- - c} \\ 0 &= (U_- - c)^2 + (U_+ - c)^2 = 2c^2 - 2(U_+ + U_-)c + U_+^2 + U_-^2 \\ c &= \frac{1}{2} \left[U_+ + U_- \pm \sqrt{(U_+ + U_-)^2 - 2(U_+^2 + U_-^2)} \right] = \frac{U_+ + U_-}{2} \pm \frac{1}{2} \sqrt{-(U_+ - U_-)^2} \\ &\equiv \bar{U} \pm i \frac{\Delta U}{2} \end{aligned} \quad (50)$$

The perturbation described by (46) and (19) propagates with a phase speed of c_r , which is the average \bar{U} of the two speeds, while it is amplified or damped at a rate c_i of $\Delta U/2$, the half-difference between the two speeds. Since c_i is always positive, the piecewise-constant profile (44) is unstable.

This simplified version of the Kelvin-Helmholtz instability yields a c which is independent of the wavenumber k : the profile (44) is unstable to perturbations with *all* wavenumbers k , which all propagate at the same speed. This unrealistic property is a consequence of the piecewise-constant profile. We now use a slightly more realistic model of the interface, in which the derivative of the velocity profile, but not the profile itself, is discontinuous at $y = \pm\delta$. The profile and the solution are described in the three regions by:

$$\begin{aligned} y > +\delta & : U = U_+ & U' = 0 & \hat{v} = \hat{v}_+ \equiv A_+ e^{-ky} & D\hat{v}_+ = -kA_+ e^{-ky} \\ -\delta < y < +\delta & : U = \bar{U} + \frac{\Delta U}{2\delta} y & U' = \frac{\Delta U}{2\delta} & \hat{v} = \hat{v}_0 \equiv A_0 e^{-ky} + B_0 e^{ky} & D\hat{v}_0 = -kA_0 e^{-ky} + kB_0 e^{ky} \\ y < -\delta & : U = U_- & U' = 0 & \hat{v} = \hat{v}_- \equiv B_- e^{ky} & D\hat{v}_- = kB_- e^{ky} \end{aligned} \quad (51)$$

When U is continuous, the condition (42) implies that \hat{v} is also. The conditions which the solution must

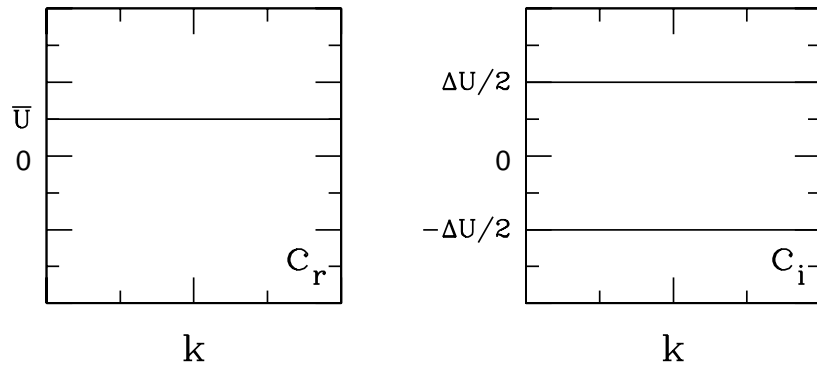


Figure 3: c_r and c_i for the Kelvin-Helmholtz instability in the case of a piecewise-constant profile.

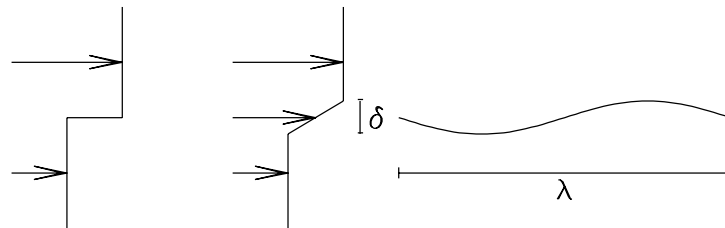


Figure 4: Left: a piecewise-constant profile. Middle: a piecewise-linear profile. Right: a piecewise-linear profile is unstable to perturbations whose wavelength λ exceeds 10δ .

satisfy are:

$$0 = \hat{v}_0(\delta) - \hat{v}_+(\delta) = A_0 e^{-k\delta} + B_0 e^{k\delta} - A_+ e^{-k\delta} \quad (52)$$

$$0 = \hat{v}_0(-\delta) - \hat{v}_-(-\delta) = A_0 e^{k\delta} + B_0 e^{-k\delta} - B_- e^{-k\delta} \quad (53)$$

$$\begin{aligned} 0 &= [(U-c)D - U']\hat{v}_0(\delta) - [(U-c)D - U']\hat{v}_+(\delta) \\ &= (U-c)[D\hat{v}_0(\delta) - D\hat{v}_+(\delta)] - [(U'\hat{v}_+(\delta)) - (U'\hat{v}_0(\delta))] \\ &= (U_+ - c)[-kA_0 e^{-k\delta} + kB_0 e^{k\delta} - (-kA_+ e^{-k\delta})] + \frac{\Delta U}{2\delta}(A_0 e^{-k\delta} + B_0 e^{k\delta}) \end{aligned} \quad (54)$$

$$\begin{aligned} 0 &= [(U-c)D - U']\hat{v}_0(-\delta) - [(U-c)D - U']\hat{v}_-(-\delta) \\ &= (U-c)[D\hat{v}_0(-\delta) - D\hat{v}_-(-\delta)] - [(U'\hat{v}_-(-\delta)) - (U'\hat{v}_0(-\delta))] \\ &= (U_- - c)[-kA_0 e^{k\delta} + kB_0 e^{-k\delta} - (kB_- e^{-k\delta})] + \frac{\Delta U}{2\delta}(A_0 e^{k\delta} + B_0 e^{-k\delta}) \end{aligned} \quad (55)$$

Using (52) and (53) to eliminate A_+ and B_- in (54) and (55) yields

$$0 = (U_+ - c)2kB_0 e^{k\delta} + \frac{\Delta U}{2\delta}(A_0 e^{-k\delta} + B_0 e^{k\delta}) \quad (56)$$

$$0 = (U_- - c)(-2k)A_0 e^{k\delta} + \frac{\Delta U}{2\delta}(A_0 e^{k\delta} + B_0 e^{-k\delta}) \quad (57)$$

or

$$\begin{bmatrix} 0 \\ 0 \end{bmatrix} = \begin{bmatrix} \frac{\Delta U}{2\delta} e^{-k\delta} & ((U_+ - c)(-2k) + \frac{\Delta U}{2\delta}) e^{k\delta} \\ ((U_- - c)2k + \frac{\Delta U}{2\delta}) e^{k\delta} & \frac{\Delta U}{2\delta} e^{-k\delta} \end{bmatrix} \begin{bmatrix} A_0 \\ B_0 \end{bmatrix} \quad (58)$$

which has a solution if and only if:

$$c = \bar{U} \pm \frac{\Delta U}{4k\delta} \sqrt{(1 - 2k\delta)^2 - e^{-4k\delta}} \quad (59)$$

Now, c depends on k and can be real (a neutral perturbation) or complex (growing or damped). The boundary between these two regimes is found by solving numerically the equation

$$(2\hat{k} - 1)^2 = e^{-2\hat{k}} \quad (60)$$

which yields $\hat{k} = 0.64$. The unstable perturbations are characterized by:

$$\begin{aligned} k\delta &< 0.64 \\ \frac{2\pi\delta}{\lambda} &< 0.64 \\ \lambda &> \frac{2\pi}{0.64} \delta \approx 10 \delta \end{aligned} \quad (61)$$

The piecewise-linear profile (51) is unstable to perturbations whose wavelength is more than 10 times the width δ of the interface. We can verify that, when δ tends to zero, we recover the previous result (50) of the discontinuous profile.

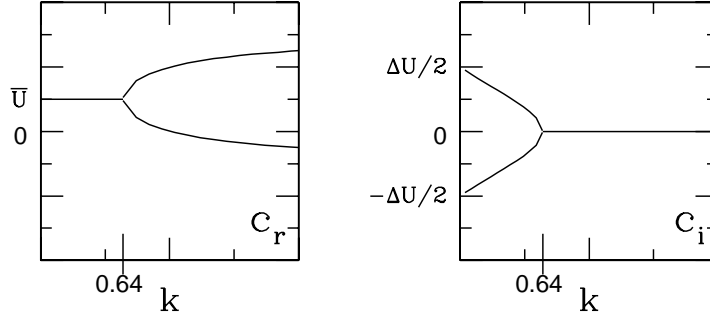


Figure 5: c_r and c_i for the Kelvin-Helmholtz instability in the case of a piecewise-linear profile.

3 Beyond eigenvalues

We return to Poiseuille and Couette flow. Poiseuille flow becomes linearly unstable at $R = R_L = 5772$ [8], whereas experiments and simulations show transition to turbulence at $R = R_T \approx 1000$. Couette flow is linearly stable for all Reynolds numbers, whereas experiments [9, 10] and simulations [11, 23] show a transition to turbulence at $R = R_T \approx 300$. Circular Poiseuille flow, or pipe flow, is also linearly stable at all R but undergoes transition to turbulence at $R = R_T \approx 2000$. For these last two flows, we can say that $R_L = \infty$.

Flow	R_T	R_L
plane Poiseuille	1000	5772
plane Couette	300	∞
pipe Poiseuille	2000	∞

In addition, turbulence is three-dimensional, unlike the two-dimensional ($\beta = 0$, i.e. independent of the transverse or spanwise direction z) perturbations shown by Squire's Theorem to be the most unstable. Many ideas have been proposed to liberate hydrodynamic stability theorem from the tyranny of Squire's Theorem and eigenvalues. In this section, we will discuss a few of these ideas. Many articles are published each year in this very active field.

3.1 Energy theory

The equation governing the evolution of the energy density is obtained by taking the scalar product of the Navier-Stokes equation with \mathbf{U} , leading to

$$\frac{\partial}{\partial t} \frac{1}{2} \mathbf{U} \cdot \mathbf{U} = \mathbf{U} \cdot \frac{\partial \mathbf{U}}{\partial t} = -\mathbf{U} \cdot [(\mathbf{U} \cdot \nabla) \mathbf{U}] - \mathbf{U} \cdot \nabla P + \frac{1}{R} \mathbf{U} \cdot \Delta \mathbf{U} \quad (62)$$

We then integrate (62) over a volume which is either periodic or with zero velocity through the boundaries. The nonlinear term is conservative, i.e. leads to zero contribution to (62). This is seen by first writing

$$\mathbf{U} \cdot [(\mathbf{U} \cdot \nabla)\mathbf{U}] = \nabla \cdot \left(\mathbf{U} \frac{U^2}{2} \right) - \frac{U^2}{2} \nabla \cdot \mathbf{U} \quad (63)$$

The second term of the right-hand-side of (63) is zero for an incompressible fluid. The first term is integrated over the volume and then transformed by Gauss's theorem. The resulting surface integral is zero because of the boundary conditions.

$$\int dV \mathbf{U} \cdot [(\mathbf{U} \cdot \nabla)\mathbf{U}] = \int dV \nabla \cdot \left(\mathbf{U} \frac{U^2}{2} \right) = \int dA \hat{\mathbf{n}} \cdot \mathbf{U} \frac{U^2}{2} = 0 \quad (64)$$

We can also calculate an analogous calculation on the *nonlinear* equations which govern the growth of a non-infinitesimal perturbation \mathbf{u} of the steady flow \mathbf{U} .

$$\mathbf{u} \cdot \partial_t \mathbf{u} + \mathbf{u} \cdot (\mathbf{u} \cdot \nabla)\mathbf{U} + \mathbf{u} \cdot (\mathbf{U} \cdot \nabla)\mathbf{u} + \mathbf{u} \cdot (\mathbf{u} \cdot \nabla)\mathbf{u} = -\mathbf{u} \cdot \nabla p + \frac{1}{R} \mathbf{u} \cdot \Delta \mathbf{u} \quad (65)$$

We substitute

$$\begin{aligned} \mathbf{u} \cdot \partial_t \mathbf{u} &= \partial_t \left(\frac{|u|^2}{2} \right) \\ \mathbf{u} \cdot [(\mathbf{u} \cdot \nabla)\mathbf{u}] &= \nabla \cdot \left(\mathbf{u} \frac{|u|^2}{2} \right) - \frac{|u|^2}{2} \nabla \cdot \mathbf{u} \\ \mathbf{u} \cdot [(\mathbf{U} \cdot \nabla)\mathbf{u}] &= \nabla \cdot \left(\mathbf{U} \frac{|u|^2}{2} \right) - \frac{|u|^2}{2} \nabla \cdot \mathbf{U} \\ -\mathbf{u} \cdot \nabla p &= -\nabla \cdot (p \mathbf{u}) + p \nabla \cdot \mathbf{u} \\ \mathbf{u} \cdot \Delta \mathbf{u} &= \nabla \cdot \nabla \left(\frac{|u|^2}{2} \right) - |\nabla \mathbf{u}|^2 \end{aligned}$$

and integrate over a volume. As previously, we use Gauss's theorem, incompressibility, and the boundary conditions (\mathbf{u} is either zero on the boundaries, or periodic) to eliminate all the terms above which are divergences. What remains is called the *Reynolds-Orr equation*:

$$\underbrace{\frac{d}{dt} \int dV \left(\frac{|u|^2}{2} \right)}_{\frac{dE(\mathbf{u})}{dt}} = \underbrace{- \int dV \mathbf{u} \cdot [(\mathbf{u} \cdot \nabla)\mathbf{U}]}_{\mathcal{P}(\mathbf{u})} - \underbrace{\frac{1}{R} \int dV |\nabla \mathbf{u}|^2}_{-\frac{1}{R} \mathcal{D}(\mathbf{u})} \quad (66)$$

$\mathcal{D}(\mathbf{u})/R$ is the energy lost by \mathbf{u} to viscous dissipation How is \mathbf{u} supplied with energy? The base flow \mathbf{U} is maintained (for example, by providing the pressure gradient for Poiseuille flow or by moving the

bounding plates for Couette flow). The term $\mathcal{P}(\mathbf{u})$ measures the energy exchanged between the base flow \mathbf{U} and the perturbation \mathbf{u} . The evolution of the energy of \mathbf{u} comes from terms which are linear in \mathbf{u} : viscous dissipation and the nonlinear term linearized about \mathbf{U} . We see that

$$\frac{1}{E(\mathbf{u})} \frac{dE(\mathbf{u})}{dt} \quad (67)$$

is independent of the amplitude of \mathbf{u} , which is a consequence of the fact that the evolution of the energy of \mathbf{u} comes from terms which are linear in \mathbf{u} .

Joseph [12] defined an critical energy Reynolds number R_E such that

- For $R < R_E$, $\dot{E}(u) < 0$ for all \mathbf{u} .
- For $R > R_E$, there exists a perturbation \mathbf{u} such that $\dot{E}(\mathbf{u}) > 0$.

It is possible to show that

$$\frac{1}{R_E} = \max_{\mathbf{u}} \left(-\frac{\mathcal{P}(\mathbf{u})}{\mathcal{D}(\mathbf{u})} \right) \quad (68)$$

Significantly, the maximum in (68) is realized for perturbations \mathbf{u} with non-zero spanwise wavenumber β . These values are shown in the table below [13].

Flow	R_E	β
plane Poiseuille	49.7	2.05
plane Couette	20.7	1.56

3.2 Transient growth

In order to explain *transient growth*. [14, 15] we consider the model problem:

$$\frac{d}{dt} \begin{bmatrix} v \\ \eta \end{bmatrix} = \begin{bmatrix} -1/R & 0 \\ 1 & -2/R \end{bmatrix} \begin{bmatrix} v \\ \eta \end{bmatrix} \quad (69)$$

Since the matrix is upper triangular, we can easily see that its eigenvalues are $-1/R$ et $-2/R$, both negative. The corresponding eigenvectors are:

$$\lambda_1 = -\frac{1}{R} : \begin{bmatrix} 1 \\ R \end{bmatrix} \quad \lambda_2 = -\frac{2}{R} : \begin{bmatrix} 0 \\ 1 \end{bmatrix} \quad (70)$$

The variables evolve as

$$\begin{bmatrix} v \\ \eta \end{bmatrix} = v_0 \begin{bmatrix} 1 \\ R \end{bmatrix} e^{-t/R} + (\eta_0 - v_0 R) \begin{bmatrix} 0 \\ 1 \end{bmatrix} e^{-2t/R} \quad (71)$$

Expand (71) for t small:

$$\begin{aligned}
\eta &= \eta_0 e^{-2t/R} + Rv_0(e^{-t/R} - e^{-2t/R}) \\
&= \eta_0 e^{-2t/R} + Rv_0\left(1 - \frac{t}{R} + \dots - 1 + \frac{2t}{R} - \dots\right) \\
&= \eta_0 e^{-2t/R} + v_0 t
\end{aligned} \tag{72}$$

Equation (72) shows that the difference between two *decreasing* exponentials can lead to algebraic *growth* over short times, a phenomenon called *transient growth*, just as is seen in Jordan blocks. We see that matrix (69) increasingly resembles a Jordan block as $R \rightarrow \infty$. This tendency can also be seen by examining the scalar product between the eigenvectors:

$$\begin{bmatrix} 1 \\ R \end{bmatrix} \cdot \begin{bmatrix} 0 \\ 1 \end{bmatrix} = R = \sqrt{1 + R^2} \cos \phi \tag{73}$$

where ϕ is the angle between the two eigenvectors. Equation (73) shows that $\phi \rightarrow 0$ and therefore that the eigenvectors become parallel as $R \rightarrow \infty$.

Even though the search for the largest (positive or least negative) eigenvalues as a function of R can be limited to $\beta = 0$, this is not the case for eigenvectors showing the largest transient growth. Returning to hydrodynamic flows, we can define:

$$G \equiv \max_{\alpha, \beta, t, \hat{v}_0, \hat{\eta}_0} \frac{E(t)}{E(0)} \tag{74}$$

where the maximum is taken over all wavenumbers α, β , all times t , and all initial conditions $\hat{v}_0(y), \hat{\eta}_0(y)$. The results are given in the table below [14, 15, 16]

Flow	G	t_{\max}	α_{\max}	β_{\max}
plane Poiseuille	$0.20 R^2 \times 10^{-3}$	$0.076 R$	0	2.04
plane Couette	$1.18 R^2 \times 10^{-3}$	$0.117 R$	$35/R$	1.6
pipe Poiseuille	$0.07 R^2 \times 10^{-3}$	$0.048 R$	0	1
Blasius boundary layer	$1.18 R^2 \times 10^{-3}$	$0.778 R$	0	0.65

The amplification factor G can be very large. For example, $G = 200$ for plane Poiseuille flow at $R = 1000$, and $G = 100$ for plane Couette flow at $R = 300$, near where transition to turbulence occurs in these flows. In addition, the perturbation which maximizes G has $\alpha = 0$ or $\alpha \rightarrow 0$. The value of β is, in the case of plane Couette flow, close to $\pi/2$, giving a half wavelength of $\pi/\beta \approx 2$, the distance between the two plates. Indeed, the perturbations with largest transient growth (called optimal perturbations) consist of longitudinal vortices, like convective rolls, whose axes are in the direction of the base flow, i.e. along x . Such structures have been observed experimentally [17, 18, 19] and numerically [20, 21].

Although these results are suggestive, the relationship between transient growth and transition to turbulence has not been demonstrated.

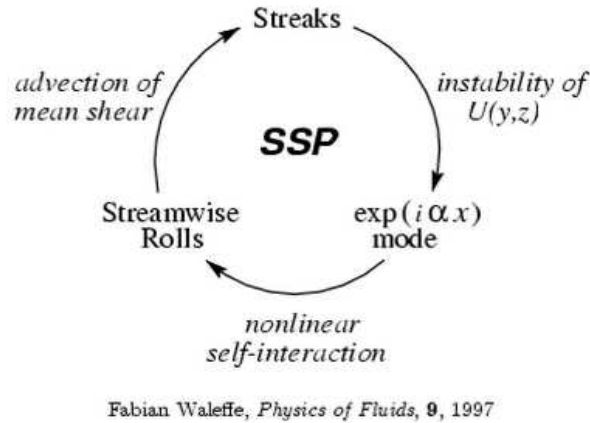


Figure 6: Self-Sustaining Process (SSP) proposed by Waleffe [22, 23, 24].

3.3 Self-Sustaining Process

From observations of numerical simulations of turbulence at low Reynolds numbers, Waleffe [22, 23, 24] proposed a theory for transitional turbulence, described in <http://www.math.wisc.edu/~waleffe/ECS/SSP.html> as follows:

This nonlinear, three-dimensional Self-Sustaining Process appears to be a generic mechanism in shear flows. The mechanism has three main elements as depicted in the figure above:

- Streamwise rolls sustain “streaks” (i.e. spanwise (z) modulation of the streamwise velocity), by redistributing the mean momentum in cross-planes,*
- the streaks suffer a wake-like instability due to the spanwise inflections that leads to the onset of a streamwise ondulation,*
- the nonlinear self-interaction of that streamwise ondulation directly regenerates the streamwise rolls.*

This process leads to self-sustained 3D traveling waves that consists of wavy streaks flanked by staggered, counter-rotating, quasi-streamwise vortices in both plane Poiseuille flow and plane Couette flow with no-slip as well as free-slip boundary conditions.

The self-sustaining process is considered to be a key ingredient in transitional shear-flow turbulence.

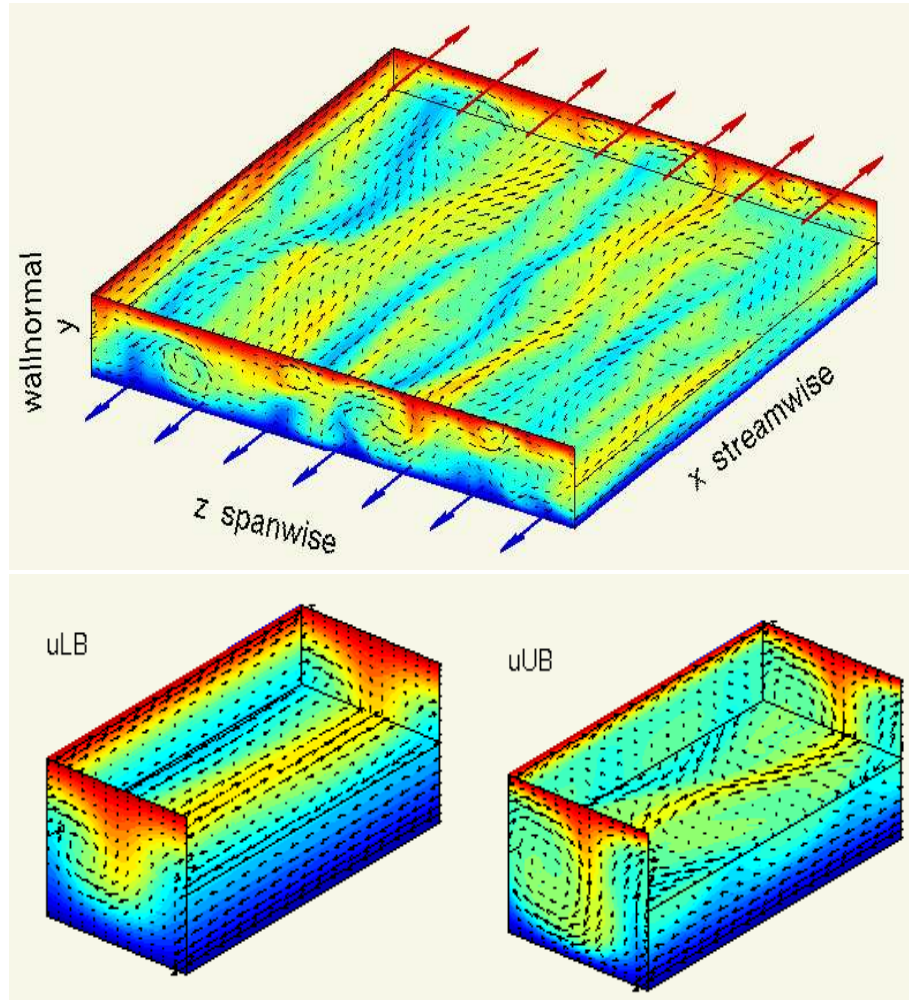


Figure 7: Three unstable steady states of plane Couette flow at $R = 400$, computed by Gibson and Cvitanovic. <http://chaosbook.org/tutorials> and <http://www.channelflow.org>

3.4 Unstable steady states and travelling waves

Until fairly recently, the only solutions known for plane Poiseuille and Couette flow and for pipe flow were the basic laminar solution and, in the case of plane Poiseuille flow, the two-dimensional Tollmien-Schlichting waves that bifurcate at $Re_L = 5772$. However, starting in 1990, large numbers of unstable solutions of wall-bounded shear flows, such as plane Couette flow [25, 26, 27, 28] and pipe Poiseuille [29, 30, 31, 32] flow have been discovered computationally. It is hypothesized that weak turbulence can be understood as chaotic trajectories that visit in turn the vicinities of the various unstable branches [33, 34, 35, 36]. In order to explain weak turbulence in wall-bounded shear flows, researchers focus on the unstable manifolds and time-dependent trajectories which connect the branches. The non-trivial solutions mostly consist of wavy longitudinal vortices ($\alpha, \beta \neq 0$) and are created via saddle-node bifurcations. The Reynolds-number threshold for weak turbulence in wall-bounded shear flows is sometimes thought to be related to the lowest of these saddle-nodes.

References

- [1] W.M.F. Orr, *The stability or instability of the steady motions of a perfect liquid and of a viscous liquid*, Proc R Irish Acad A **27**, 9 (1907).
- [2] A. Sommerfeld, *Ein Beitrag zur hydrodynamischen Erklärung der turbulenten Flüssigkeitsbewegungen*, In Atti. del 4 Congr. Internat. dei Mat. III, 116–124 (1908).
- [3] H.B. Squire, *On the stability for three-dimensional disturbances of viscous fluid flow between parallel walls*, Proc. Roy. Soc. Lond. Ser. A **142**, 621 (1933).
- [4] L. Rayleigh, *On the stability of certain fluid motions* Proc. Math. Soc. Lond. **11**, 57 (1880).
- [5] L. Rayleigh, *On the stability of certain fluid motions*, Proc. Math. Soc. Lond. **19**, 67 (1887).
- [6] R. Fjortoft, *Application of integral theorems in deriving criteria for instability for laminar flows and for the baroclinic circular vortex*, Geofys Publ. Oslo **17**, 1 (1950).
- [7] L. Howard, *Note on a paper of John W. Miles*, J. Fluid Mech. **10**, 509 (1961).
- [8] S.A. Orszag, *Accurate solution of the Orr-Sommerfeld stability equation*. J. Fluid. Mech. **50**, 689 (1971).
- [9] N. Tillmark & P.H. Alfredsson, *Experiments on transition in plane Couette flow*, J. Fluid Mech. **235**, 89 (1992).
- [10] F. Daviaud, J. Hegseth, & P. Bergé, *Subcritical transition to turbulence in plane Couette flow*, Phys. Rev. Lett. **69**, 2511 (1992).
- [11] A. Lundbladh & A.V. Johansson, *Direct simulation of turbulent spots in plane Couette flow*, J. Fluid Mech. **229**, 499 (1991).
- [12] D.D. Joseph, *Stability of Fluid Motions I, II*. Springer, 1976.
- [13] S.C. Reddy & D.S. Henningson, *Energy growth in viscous channel flows*, J. Fluid Mech. **252**, 209 (1993).
- [14] K.M. Butler & B.F. Farrell, *Three-dimensional optimal perturbations in viscous shear flow*, Phys. Fluids A **4**, 1637 (1992).
- [15] L.N. Trefethen, A.E. Trefethen, S.C. Reddy, & T.A. Driscoll, *Hydrodynamic stability without eigenvalues*, Science **261**, 578 (1993).
- [16] P.J. Schmid & D.S. Henningson, *Optimal energy density growth in Hagen-Poiseuille flow*. J. Fluid Mech. **277**, 197 (1994)
- [17] O. Dauchot & F. Daviaud, *Streamwise vortices in plane Couette flow*, Phys. Fluids **7**, 901 (1995).
- [18] S. Bottin, O. Dauchot & F. Daviaud, *Intermittency in a locally forced plane Couette flow*, Phys. Rev. Lett. **79**, 4377 (1997).

- [19] S. Bottin, O. Dauchot, F. Daviaud, & P. Manneville, *Experimental evidence of streamwise vortices as finite amplitude solutions in transitional plane Couette flow*, Phys. Fluids **10**, 2597 (1998).
- [20] D. Barkley & L.S. Tuckerman, *Stability analysis of perturbed plane Couette flow*, Phys. Fluids **11**, 1187 (1999).
- [21] L.S. Tuckerman & D. Barkley, *Symmetry breaking and chaos in perturbed plane Couette flow*, Theoret. Comput. Fluid Dynamics **16**, 91 (2002).
- [22] F. Waleffe, *Proposal for a Self-Sustaining Mechanism in Shear Flows*, Center for Turbulence Research, Stanford University/NASA Ames, Spring 1990. Unpublished.
- [23] J.M. Hamilton, J. Kim, & F. Waleffe, *Regeneration mechanisms of near-wall turbulence structures*, J. Fluid Mech. **287**, 317 (1995).
- [24] F. Waleffe, *On a self-sustaining process in shear flows*, Phys. Fluids **9**, 883–900 (1997).
- [25] M. Nagata, *Three-dimensional finite-amplitude solutions in plane Couette flow: bifurcation from infinity*, J. Fluid Mech. **217** (1990).
- [26] G. Kawahara, S. Kida, *Periodic motion embedded in plane Couette turbulence: regeneration cycle and burst*, J. Fluid Mech. **449**, 291 (2001).
- [27] F. Waleffe, *Homotopy of exact coherent structures in plane shear flows*, Phys. Fluids **15** (2003).
- [28] J. Halcrow, J.F. Gibson, P. Cvitanović, *Equilibrium and traveling-wave solutions of plane Couette flow*, J. Fluid Mech. **638**, 243–266 (2009).
- [29] B. Hof, C.W.H. van Doorne, J. Westerweel, F.T.M. Nieuwstadt, H. Faisst, B. Eckhardt, H. Wedin, R.R. Kerswell, F. Waleffe, *Experimental Observation of Nonlinear Traveling Waves in Turbulent Pipe Flow*, Science **305**, 1594–1598 (2004).
- [30] H. Faisst and B. Eckhardt, *Traveling waves in pipe flow* Phys. Rev. Lett. **91**, 22 4502 (2003).
- [31] H. Wedin and R. Kerswell, *Exact coherent structures in pipe flow: travelling wave solutions*, J. Fluid Mech. **508**, 333–371 (2004).
- [32] B. Eckhardt, T.M. Schneider, B. Hof, J. Westerweel, *Annu. Rev. Fluid Mech.* **39**, 447–468 (2007).
- [33] J. Jimenez, G. Kawahara, M. Simens, M. Nagata, *Characterization of near-wall turbulence in terms of equilibrium and bursting solutions*, Phys. Fluids **17**, 01 5105 (2005).
- [34] J. Wang, J. Gibson, F. Waleffe, *Lower branch coherent states in shear flows: transition and control*, Phys. Rev. Lett. **98**, 20 4501 (2007).
- [35] Y. Duguet, A.P. Willis, R.R. Kerswell, *Transition in pipe flow: the saddle structure on the boundary of turbulence*, J. Fluid Mech. **613**, 255-274 (2008).
- [36] J. F. Gibson, J. Halcrow, P. Cvitanović, *Visualizing the geometry of state space in plane Couette flow*, J. Fluid Mech. **611**, 107–130 (2008).